Available online www.jocpr.com

Journal of Chemical and Pharmaceutical Research, 2018, 10(11): 63-75

Research Article

ISSN : 0975-7384
CODEN(USA) : JCPRC5

An Improved Study on Molecular Structure, Fundamental Vibrations and Optical Property of Novel Pyrimidine Derivative

T Velavan[1], A Dhandapani[2], C Adaikalaraj[3], S Manivarman[1*]

[1]*Department of Chemistry, Government Arts College, C. Mutlur, Chidambaram 608102, Tamil Nadu, India*
[2]*CK College of Engineering and Technology, Cuddalore 607 003, Tamil Nadu, India*
[3]*Department of Chemistry, St. Joseph's College of Arts and Science, (Autonomous) Cuddalore-607001, Tamil Nadu, India*

ABSTRACT

A new Biginelli compound was synthesized by multi component reaction method and it was characterized by FT-IR, FT-Raman and NMR spectral analysis. The molecular structure and optical property of the synthesized compound were analysed by theoretical method using DFT/B3LYP-6-31G(d,p) level of theory. The experimental wavenumbers supported by calculated wavenumber, most of the vibrations show good agreement with each other. The charge transfer interactions were analysed by frontier molecular orbitals. NLO calculations were conducted to obtain the electric dipole moment and polarizability of the title compound, from the results the studied compound have higher hyperpolarizability then standard urea. In addition to this, molecular electrostatic potential have been analysed to find the most reactive region in the studied compound.

Keywords: DFT; NLO; MEP; FT-IR; FT-raman

INTRODUCTION

Pyrimidine and pyrimidine-based compounds play diverse roles in chemistry. A library of pyrimidine derivatives was designed, synthesized and studied for their usage in the medicinal area [1-4]. They show several biological activities including anti-hypertensive, antioxidant, antiviral, antifungal, anticonvulsant, inflammatory, anticancer and antibacterial. Various pyrimidine derivatives are still being used as medicines, e.g., stavudine as an anti-HIV agent, fervennuline as an antibiotic, minoxidil as an antihypertensive agent. Dihydropyrimidines and its derivatives can act as antagonists of allergic or solid tumours [5,6], antifilarial agents [7], inhibitors of cancer cells [8] and DNA modificators [9,10]. The pyrimidine-based compounds have a potential to be a newer therapeutic agents candidate. Because of this, new synthesis methods are developed as well as the methods for biological evaluation. The activity of heterocyclic compounds can be improved by fusing the pyrimidine analogs with different heterocyclic moieties [4].

Pyrimidine-based materials are also valued for their optical and physical properties. They were used as an inhibitor of corrosion of metal surfaces [11, 12], as luminescent materials [13] and as fluorescent ratiometric chemosensors [14]. Besides detailed experimental studies of pyrimidine derivatives, theoretical studies based on DFT calculations

shed light their structures, spectroscopic assignments, tautomeric studies and reaction mechanisms etc. [11,15-18]. Herein, based on the above factor, we synthesized Ethyl 6-methyl-4-(3-nitrophenyl)-2-oxo-1,2,3,4-tetrahydropyrimidine-5-carboxylate (EMNTC), to study some spectroscopic and structural properties of the compound in combination with theoretical calculations. To the best of our knowledge, there is no any information related to X-ray and DFT studies in the literature. In this study, the molecular geometry, vibrational spectra, frontier molecular orbitals, MEP map and global reactivity descriptors of the molecule were studied to get further information about the molecule.

COMPUTATIONAL DETAILS

Gaussian 03 quantum chemical software [19] was used in all calculations of the studied molecule. Optimized structural parameters and vibrational wave numbers for the molecule were calculated by using B3LYP/6-31G (d, p) level of theory. The vibrational modes were assigned on the basis of potential energy distribution analysis using VEDA4 program [20]. The calculated harmonic vibrational wave numbers were scaled down uniformly by a factor of 0.9608 for B3LYP/6-31G (d, p) level of theory, which accounts for systematic errors caused by basis set incompleteness, neglect of electron correlation and vibrational anhormonicity [21-23].

EXPERIMENT

Synthesis of Ethyl 6-Methyl-4-(3-Nitrophenyl)-2-oxo-1,2,3,4-Tetrahydropyrimidine-5-Carboxylate (I)

Ethanolic mixture of 3-nitro-benzaldehyde (0. 6 mmol), ethyl acetoacetate (0. 9 mmol) and urea (0. 9 mmol) were stirred in Con. Hydrochloric acid in condensation vessels. The reaction mixture was refluxed at 80^{o}C for 12h. Completion of the reaction was monitored by thin layer chromatography. The crude content was cooled and poured into crust-ice, the obtained solid product were filtered and washed with ethanol. The crude product was recrystallized from absolute ethanol. Yield: 73%, melting point=218 ^{o} C (Scheme 1).

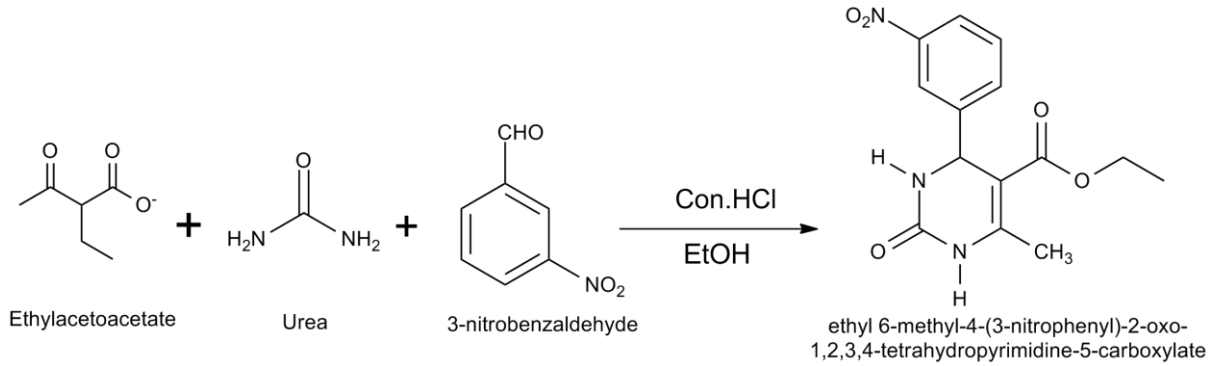

Scheme 1

RESULT AND DISCUSSION

Vibrational Assignment

The vibrational analysis of EMNTC was performed on the basis of the characteristic vibrations of methyl, carbonyl, carbonyl and methine. The molecule under consideration belongs to the C1 point group. In order to obtain the spectroscopic signature of the investigated molecule, frequency calculation analysis has been performed by DFT method using B3LYP/6-31G(d,p) level of theory. The computed harmonic wavenumbers and their intensities of FT-IR and FT-Raman corresponding to the different normal modes are used for identifying the vibrational modes unambiguously. The optimized structure of EMNTC is shown in Figure 1. The calculated wavenumbers are compared with the experimental FT-IR and FT-Raman bands are summarised in Table.1 along with their PED contribution, intensities and force constants. The recorded FT-IR and FT-Raman spectrums are shown in Figures 2 and 3.

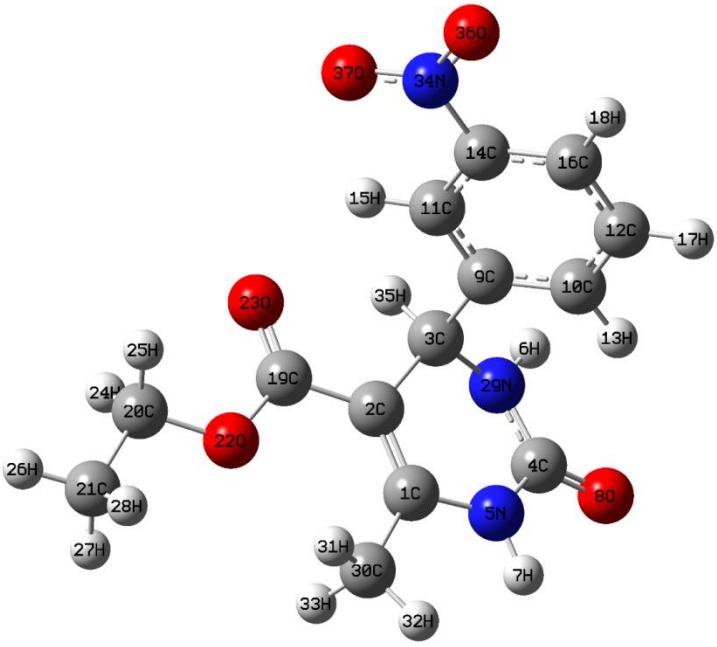

Figure 1. The Optimized structure of EMNTC

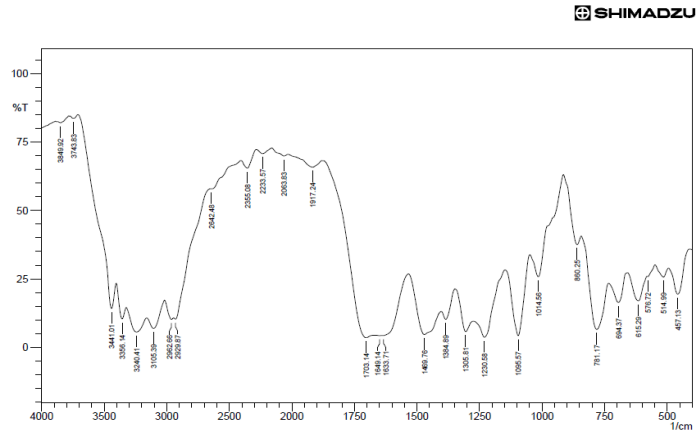

Figure 2. The FT-IR Spectrum of EMNTC

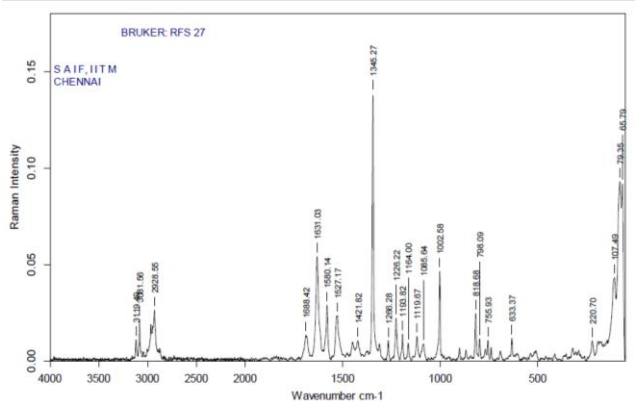

Figure 3. The FT-Raman Spectrum of EMNTC

N-H and C-N Vibrations

In the FT-IR spectra of EMNTC, the N–H stretching of Pyrimidine ring is observed at 3441 cm-1, whereas this is calculated at 3507 and 3496 cm-1 shows good agreement with each other. The deformation vibrations calculated at 1441 and 1440 cm-1.

The identification of C–N, C–N vibrations is very difficult task, since the mixing of several bands are possible in these regions. Silverstein et al. [24] assigned the C–N stretching absorption in the region 1382–1266 cm-1. In the present study, the band observed at 1230 cm-1 in FT-IR spectrum and 1226, 1421cm-1 in FT-Raman spectrum are assigned to C–N stretching vibration. These vibrations calculated at 1441, 1358 and 1237 cm-1. The in-plane and out-of-plane bending vibrations of carbon-nitrogen group are assigned in this study which are also supported by the literature [25].

C-H vibrations

Since the title molecule is a substituted heterocyclic aromatic system, it has only four C–H moiety. The substituted benzene gives rise to C–H stretching, C–H in-plane bending and C–H out-of plane deformations. The hetero aromatic structure shows the presence of C–H stretching vibrations in the region 3000–3100 cm^{-1} which is the characteristic region for the ready identification of such stretching vibrations [26]. In this region, the bands are not affected, appreciably by the nature of the substituents. Hence, in this study, the C–H vibrations of the title molecule are observed at 3105 cm^{-1} in FT-IR spectrum and 3119, 3081 cm^{-1} in FT-Raman and show good agreement with the calculated results 3126, 3118, 3095 and 3078cm^{-1}. The FT-IR band at 1095 cm^{-1} is assigned to C–H in-plane bending vibrations of the title molecule. The C–H out-of-plane bending vibrations are calculated at 964, 940 and 920 cm^{-1}. The aliphatic C–H stretching vibration observed at 2962 in FT-IR spectrum and shows good agreement calculated wavenumber at 2981 cm^{-1}.

C=O vibration

The C=O stretching frequency appears strongly in the IR spectrum in the range of 1600-1850 cm^{-1}, because of its large change in dipole moment. The carbonyl group vibrations give a rise to characteristic bands in vibration spectra and its characteristic frequency is used to study a wide range of compounds. The intensity of these bands can increase depending on the conjugation or formation of hydrogen bonds . In the present study, a very strong absorption band is observed at 1703, 1649 cm^{-1} in FT-IR spectrum and 1688 cm^{-1} in FT-Raman spectrum. These

vibrations show good agreement with calculated wavenumber at 1761 and 1683 cm^{-1}. The deformation vibrations observed at 755 cm^{-1}.

Nitro group (NO_2) vibrations

Among various aromatic compounds, molecules with aromatic nitro group have numerous pharmacological applications and utilized as strong coordinating group in organic synthesis. Aromatic nitro compounds have strong absorption due to the asymmetric and symmetric stretching vibrations at 1625–1510 cm^{-1} and 1400–1360 cm^{-1} respectively [27]. The very strong bands of NO2 group are appeared at 1614 cm^{-1} in FT-IR spectrum and 1580 cm^{-1} in FT-Raman spectrum and the calculated wavenumbers 1614 and 1574 cm^{-1}indicates great concurrence with the experimental values. The symmetric stretching vibrations observed at 1345 in FT-Raman perfectly coincide with computed wavenumber at 1346 cm^{-1}. The introduction of NO2 group in the pi-conjugated materials can remarkably enhance the intramolecular charge transfer from donor to the acceptor moieties which results in the alteration of dipole moment, thus gaining a strong infrared activity.

Table 1. The vibrational assignments of EMNTC using PED

Sl.No	Unscaled	Scaled	FT-IR	FT-Raman	Red. Mass	Force Constant	IR intensity	Raman intensity	PED
1	3646	3507			1.08	8.44	12.96	1.95	νN5H7(99)
2	3634	3496	3441		1.08	8.38	7.76	1.61	νN29H6(99)
3	3250	3126			1.09	6.8	0.31	2.49	νC16H18(97)
4	3241	3118	3105	3119	1.09	6.76	2.98	1.11	νC11H15(99)
5	3217	3095		3081	1.09	6.67	0.92	2.17	νC10H13(100)+ νC12H17(98)
6	3199	3078			1.09	6.56	1.09	2.19	νC10H13(100)+ νC12H17(98)
7	3183	3062			1.1	6.55	0.44	0.98	νC30H31(99)
8	3138	3019			1.11	6.41	6.48	0.39	νC20H24(98)+ νC20H25(99)+ νC21H27(99)+ νC21H28(100)
9	3131	3012			1.1	6.37	3.95	3.06	νC21H26(98)+ νC21H27(99)+ νC21H28(100)
10	3124	3005			1.1	6.34	2.49	2.15	νC30H32(92)+ νC30H33(96)
11	3111	2993			1.11	6.32	0.44	2.39	νC20H24(98)+ νC20H25(99)+ νC21H27(99)+ νC21H28(100)
12	3099	2981	2962		1.09	6.14	0.51	1.67	νC3H35(99)
13	3071	2955	2929	2928	1.06	5.88	2.71	2.5	νC20H24(98)+ νC20H25(99)
14	3061	2945			1.04	5.75	2.69	5.1	νC30H31(99)+ νC30H32(92)+ νC30H33(96)
15	3056	2939			1.04	5.7	2.63	3.92	νC21H26(98)+ νC21H27(99)+ νC21H28(100)
16	1830	1761	1703		7.68	15.15	100	1.97	νO8C4(73)
17	1749	1683	1649	1688	12.05	21.72	60.43	7.21	νO23C19(84)
18	1681	1617	1633	1631	7.55	12.57	30.4	7.06	νC1C2(70)
19	1677	1614			8.09	13.41	5.97	0.83	νO36N34(79)+ νO37N34(80)+ νC11C14(42)+ νC14C16(47)+ νC10C12(45)

20	1636	1574		1580	6.43	10.13	5.62	5.51	νC12C16(51)+ β C11C14C16(50)
21	1626	1564		1527	8.28	12.9	27.99	2.97	νO36N34(79)+ νO37N34(80)+ νC9C10(52)
22	1533	1475			1.09	1.51	0.95	0.18	β H24C20H25(79)+ β H27C21H28(83)+ ΓC20H24C21H25(84)
23	1522	1465	1469		2.35	3.22	1.93	0.2	β H13C10C9(59)+ β H15C11C9(79)+ β H17C12C10(57)
24	1513	1455			1.05	1.42	0.19	2.34	β H24C20H25(79)+ β H27C21H28(83)
25	1505	1448			1.12	1.49	2.04	2.19	β H31C30H33(67)+ β H32C30C1(54)+ ΓC30H32H33H31(77)
26	1503	1446			1.04	1.39	1.12	3.46	β H26C21H27(81)+ τ SH27C21C20O22(34)+ τ SH28C21C20O22(50)
27	1498	1441		1421	1.9	2.51	14.02	3.49	νN5C1(39)+ β H7N5C4(57)+ β H32C30H33(78)
28	1482	1426			1.36	1.76	1.78	2.45	β H32C30H33(78)
29	1479	1423[a]			1.96	2.53	12.55	1.54	νC11C14(42)+ β H18C16C14(65)+ β H13C10C9(59)+ β H32C30H33(78)
30	1455	1400[c]			1.85	2.31	13.7	2.44	β H6N29C3(57)+ ΓC3C9N29H35(56)
31	1439	1385[d]	1384		1.44	1.75	1.77	1.47	β H26C21C20(56)+ β H27C21H28(83)+ ΓC20H24C21H25(84)+ τ H28C21C20O22(50)
32	1430	1376			1.23	1.48	2.29	2.77	β H31C30H33(67)+ ΓC30H32H33H31(77)
33	1411	1358			2.09	2.45	5.38	0.74	νN5C4(47)+ β H6N29C3(57)+ β H35C3C9(74)
34	1409	1356			1.49	1.74	7.55	1.05	β H26C21C20(56)+ β H27C21H28(83)+ ΓC20H24C21H25(84)
35	1399	1346		1345	12.98	14.97	50.64	25.96	νO36N34(79)+ νO37N34(80)+ β O36N34O37(60)
36	1369	1317	1305		3.51	3.88	4.4	0.57	νC14C16(47)+ νC9C10(52)+ β H35C3C9(74)
37	1352	1300			2.93	3.16	30.5	3.43	νC19C2(31)+ β C1C2C3(32)+ ΓC20H24C21H25(84)
38	1345	1294			1.54	1.65	8.33	0.56	β H18C16C14(65)+ β H35C3C9(74)+ β H15C11C9(79)
39	1306	1257		1266	1.58	1.59	0.73	0.43	νC9C10(52)+ β H35C3C9(74)+ β H13C10C9(59)+ β H15C11C9(79)
40	1298	1248			1.1	1.09	0.1	2.67	β H24C20C21(91)

41	1285	1237	1230	1226	2.23	2.17	7.93	1.16	νN5C1(39)+ β H7N5C4(57)
42	1266	1218		1193	2.35	2.22	80.58	2.68	ΓC3C9N29H35(56)
43	1215	1169		1164	2.01	1.75	0.94	3.65	νC3C9(52)+ β C10C9C11(29)+ β H13C10C9(59)
44	1195	1150			1.59	1.33	0.73	3.63	νC10C12(45)+ νC3C9(52)+ β H18C16C14(65)+ β H17C12C10(57)
45	1184	1139		1119	1.54	1.27	0.73	0.38	β H26C21H27(81)+ ΓC20C21O22H24(82)+ τ H24C20C21H26(76)+ τ H27C21C20O22(34)
46	1151	1107			2.54	1.98	2.96	0.27	νC30C1(22)+ νN29C3(34)+ β C4N29C3(21)
47	1145	1101			2.84	2.19	3.87	2.68	νO22C19(36)+ νC21C20(60)+ β C21C20O22(67)
48	1131	1088	1095		3.15	2.37	12.27	0.56	β H35C3C9(74)+ β H13C10C9(59)
49	1127	1084		1085	1.91	1.43	4.21	3.11	νC12C16(51)+ β H13C10C9(59)+ β H15C11C9(79)
50	1111	1069			1.6	1.16	8.43	0.72	νC11C14(42)+ νC14C16(47)+ νC10C12(45)+ β H18C16C14(65)+β H15C11C9(79)
51	1103	1061			3.13	2.24	48.83	0.84	νO22C19(36)+ νN29C3(34)+ νO22C20(63)
52	1057	1017	1014		1.54	1.01	1.55	0.33	β H32C30H33(78)+ ΓC30H31C1H32(69)+ ΓC30C2N5C1(55)
53	1044	1004		1002	2.5	1.6	0.53	1.75	νC21C20(60)+ νO22C20(63)+ β H32C30C1(54)
54	1021	982			1.93	1.19	3.58	0.21	νC21C20(60)+ β H32C30C1(54)
55	1017	978			6.16	3.75	0.01	9.18	νC14C16(47)+ β C11C14C16(50)+ β C14C16C12(15)+ β C10C12C16(43)
56	1002	964			1.31	0.78	0.02	0.13	τ H18C16C12C10(61)+ ΓC10C9C12H13(72)+ ΓC12C10C16H17(80)
57	977	940			1.4	0.79	2.56	0.92	ΓC11C9C14H15(85)
58	957	920			2.1	1.13	0.2	0.28	νN5C4(47)+ τ H18C16C12C10(61)+ ΓC10C9C12H13(72)
59	947	911			1.9	1.01	0.89	0.39	νN5C4(47)+ τ H18C16C12C10(61)+ ΓC10C9C12H13(72)+ ΓC11C9C14H15(85)
60	918	883			4.88	2.42	2.35	0.64	νN34C14(45)+ νC3C9(52)+ β O36N34O37(60)
61	887	853	8 60		2.72	1.26	2.45	5.11	νO22C20(63)+ β

									H26C21C20(56)
62	857	824		818	6.5	2.81	0.81	0.4	νO22C19(36)+ β O22C19O23(45)
63	839	808			2.3	0.96	1.27	2.19	τ H18C16C12C10(61)+ ΓC12C10C16H17(80)
64	822	791	781	798	3.35	1.33	2.16	2.69	β O36N34O37(60)+ ΓC12C10C16H17(80)
65	814	783			1.15	0.45	0.06	0.28	β H24C20C21(91)+ ΓC20C21O22H24(82)
66	802	772			4.75	1.8	1.22	4.06	β C4N29C3(21)
67	766	737		755	8.4	2.9	2.53	1.11	ΓO23C2O22C19(56)
68	756	727			8.8	2.96	10.27	1.15	ΓO37C14O36N34(58)+ ΓO8N5N29C4(78)
69	746	718			4.69	1.54	5.77	2.14	ΓO37C14O36N34(58)+ ΓO8N5N29C4(78)
70	710	683	694		2.95	0.88	2.82	0.7	τ C11C14C16C12(46)+ τ C11C9C10C12(49)
71	697	671			5.15	1.48	2.5	0.9	β O36N34O37(60)+ β C10C12C16(43)+ τ C11C9C10C12(49)
72	669	644		633	4.25	1.12	1.53	1.15	τ H7N5C4N29(83)
73	641	617	615		4.84	1.17	1.56	1.89	β N5C4N29(24)+ β N29C3C9(31)
74	632	608			3.8	0.89	3.87	2.01	β N5C4O8(47)
75	616	593	576		1.75	0.39	22.06	1.64	τ H7N5C4N29(83)+ τ H6N29C4N5(74)
76	556	535			2.75	0.5	4.82	1.73	τ H7N5C4N29(83)+ ΓC30C2N5C1(55)
77	552	531			2.74	0.49	3.21	1.16	β O36N34C14(64)+ τ H6N29C4N5(74)
78	538	518	514		2.03	0.35	0.33	3.03	β O36N34C14(64)+ τ H7N5C4N29(83)+ τ H6N29C4N5(74)
79	514	494			3.95	0.61	0.41	3.49	νN5C4(47)+ νC30C1(22)+ β C1N5C4(26)+ τ H7N5C4N29(83)
80	511	492			3.95	0.61	1.34	0.99	β N5C4N29(24)+ τ C11C14C16C12(46)+ τ C11C9C10C12(49)
81	447	430	457		5.81	0.68	1.95	0.65	β N5C4O8(47)+ β O22C19C2(36)+ β C21C20O22(67)
82	441	424			3.57	0.41	0.12	0.12	τ C11C14C16C12(46)+ τ C10C12C16C14(53)
83	416	400			7.13	0.73	0.11	0.56	νN34C14(45)+ β C11C14C16(50)
84	394	379			4.78	0.44	0.98	1.94	β O22C19O23(45)+ β C21C20O22(67)
85	377	363			5.79	0.49	0.05	2.9	ΓC19C1C3C2(40)
86	346	333			3.34	0.24	1.14	0.63	β C2C1C30(54)
87	321	309			6.61	0.4	0.28	2.93	νC3C9(52)+ β

									C10C9C11(29)+ β O36N34C14(64)
88	302	291			4.75	0.26	1.77	4.17	νC19C2(31)+ β C1C2C3(32)+ β C20O22C19(39)
89	295	283			5.92	0.3	0.17	0.9	β C3C9C11(48)+ β N29C3C9(31)+ β C11C14N34(48)
90	275	264			1.3	0.06	0.24	0.25	τ H24C20C21H26(76)+ τ H28C21C20O22(50)
91	247	237		220	4.43	0.16	1.07	1.26	β C3C2C19(39)+ β C21C20O22(67)
92	217	209			4.54	0.13	0.43	5.71	ΓC19C1C3C2(40)+ τ C3C9C10C12(50)
93	179	173			5.22	0.1	0.85	2.19	τ C9C11C14N34(60)
94	166	160			4.26	0.07	0.61	4.15	τ C2C1N5C4(43)+ τ C9C11C14N34(60)+ ΓC30C2N5C1(55)
95	148	142			7.14	0.09	0.4	5.48	β C3C9C11(48)+ β C11C14N34(48)
96	136	131			2.25	0.02	0.13	2.35	β C20O22C19(39)+ τ H33C30C1N5(75)+ τ C20O22C19C2(65)
97	122	117		107	2.15	0.02	0.15	2.06	τ H33C30C1N5(75)+ τ C20O22C19C2(65)
98	99	95			8.14	0.05	0.13	0.36	τ C3C2C19O22(80)+ τ C21C20O22C19(95)+ ΓC19C1C3C2(40)
99	84	81			1.84	0.01	0.08	2.27	β O22C19C2(36)+ β C3C2C19(39)+ τ H33C30C1N5(75)
100	74	71			4.02	0.01	0.06	11.04	τ C4N29C3C9(30)+ τ C21C20O22C19(95)
101	65	63			4.76	0.01	0.26	19.84	τ C11C14N34O36(87)+ τ N5C4N29C3(34)+ τ C3C9C10C12(50)
102	60	58			3.47	0.01	0.04	14.78	τ C1C2C3C9(22)+ τ C21C20O22C19(95)
103	45	43			9.44	0.01	0.03	43.35	τ C11C14N34O36(87)+ τ C3C9C10C12(50)
104	26	25			4.26	0	0.09	23.46	τ C3C2C19O22(80)+ τ C21C20O22C19(95)
105	15	14			6.37	0	0.19	100	τ N29C3C9C11(75)

[v]: Stretching, δ: in-plane-bending, Γ: out-of-plane bending, vw: very weak, w: weak, m: medium, s: strong, vs: very strong,

[a]Scaling factor: 0.9608,b Relative IR absorption intensities normalized with highest peak absorption equal to 100,

[c]Relative Raman intensities calculated by Equation and normalized to 100.

[d]Potential energy distribution calculated at B3LYP/6-311++G(d,p) level

HOMO and LUMO Analysis

The analysis of the wave function indicates that the electron adsorption corresponds to the transition from the ground state to the first excited state and is mainly described by one-electron excitation from the highest occupied molecular orbital (HOMO) to the lowest unoccupied molecular orbital. The energy gap between HOMO and LUMO

(ΔEH–L) characterizes the molecular chemical stability and it is a critical parameter in determining molecular electrical transport properties.

In this study, the investigated molecule is predicted to be more stable. Our results reveal clearly that the HOMO is located over pyrimidine ring and LUMO located over phenyl ring of the studied compound, which is shown in Figure 4. Therefore, the HOMO–LUMO energy gaps of the compound with lower energy indicate the molecule is kinetically stable. Other global descriptors calculated from the frontier molecular orbital energies, such as electrophilicity index and max. Charge transfer capability, global hardness and electronic chemical potential, provide very useful information related to the physical and physicochemical properties of the molecule.

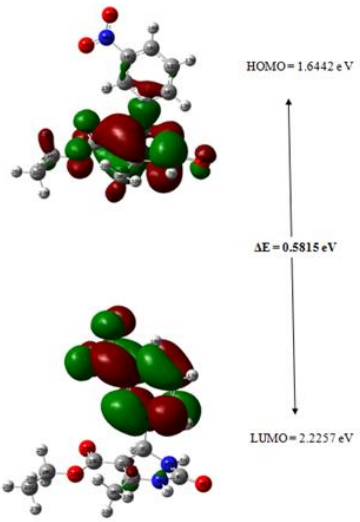

Figure 4. The Frontier molecular orbitals of EMNTC

At this point, the smaller energy gap and global hardness values mean the more reactive molecule; electrophilicity index in terms of the electronic chemical potential and global hardness represents the capability of the molecule to accept the electrons from a donor environment. As known well, in according with Koopmans Theorem [28], the Ionization energy (I) and electron affinity (E) can be expressed through HOMO and LUMO orbital energies [29]. Also, Parr R.G. and co-workers [30] have defined the DFT based global descriptors which are electronic chemical potential (χ), global hardness (η), electrophilicity (ω) are reported in the table 2.

Table 2. The Global reactivity descriptors of EMNTC

Global reactivity descriptors	Values (eV)
HOMO	1.6442
LUMO	2.2257
energy gap (ΔE)=HOMO–LUMO	-0.5815
ionization energy I=–E_{HOMO}	-1.6442
electron affinity A=–E_{LUMO}	-2.2257
Global hardness (η)=1/ 2(E_{LUMO}– E_{HOMO})	0.8598
Global softness (s)=S=1/ 2η	0.5815
Electronegativity (χ)=–1/ 2(E_{LUMO}+ E_{HOMO})	-0.1292
Chemical potential (μ)=- χ	0.1292
global electrophilicity index (Ψ)=μ^2/ 2η	0.00965

Molecular Electrostatic Potential

To get information about the nucleophilic or electrophilic region of EMNTC, the molecular electrostatic potential surface map was obtained at B3LYP/6-31G(d,p) level (Figure 5). The molecular electrostatic potential has been used for predicting relative reactivities towards electrophilic and nucleophilic attack as well as biological recognition and hydrogen bonding interactions [31,32]. The electrostatic potentials increase from red to blue color region, i.e., the regions red in color exhibit nucleophilic sites while the blue regions electrophilic sites. From the MEP of the molecule, the positive and negative potential sites occur around hydrogen atoms and over nitrogen (N_1) and sulphur atoms, respectively.

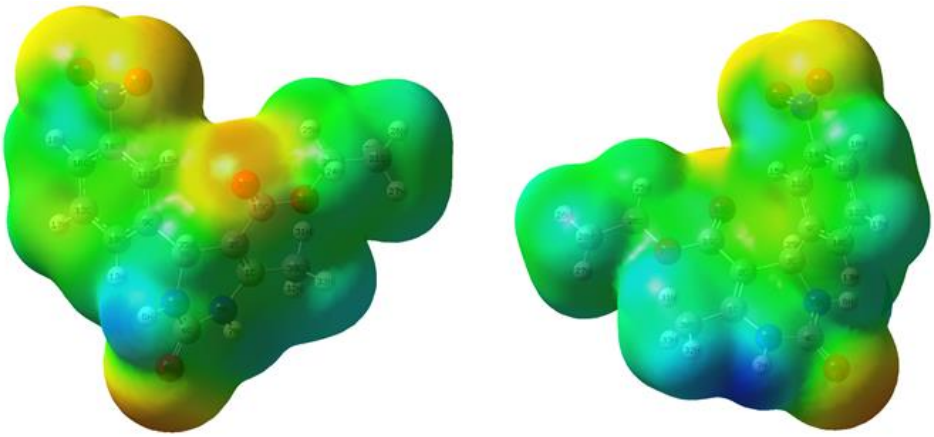

Figure 5. The Molecular Electrostatic Potential of EMNTC

Nonlinear Optical Properties

The NLO activity provides the key functions for optical modulation and switching, frequency shifting and optical logic for the developing technologies in areas such as communication, signal processing and optical inter connections [33,34]. Organic molecules able to manipulate photonic signals efficiently are of importance in technologies such as optical communication, optical computing, and dynamic image processing [35, 36]. In this context, the dynamic first hyperpolarizability of the EMNTC compound is also calculated in the present study. The first hyperpolarizability (β_0) of this novel molecular system is calculated using DFT method, based on the finite field approach. In the presence of an applied electric field, the energy of the calculated first hyperpolarizability of the title compound is 5.886 x 10^{-30} esu**.** The calculated hyperpolarizability of the title compound is 45.27 times greater than that of the standard NLO material urea (0.13 × 10^{-30} esu) [37], which is tabulated in Table. 3. We conclude that the EMNTC compound is an attractive object for future studies of nonlinear optical properties.

Table 3. The Non-Linear Optical properties of EMNTC

Parameters	**B3LYP/6-31G(d,p)**
Dipole moment (μ) Debye	
μ_x	1.8616
μ_y	0.4345

μ_z	0.8886
μ	2.1080 Debye
Polarizability (α_0) x10^{-30}esu	
α_{xx}	198.15
α_{xy}	11.38
α_{yy}	221.18
α_{xz}	-1.87
α_{yz}	19.06
α_{zz}	124.19
α	0.460 x10^{-30} esu
Hyperpolarizability (β_0) x10^{-30}esu	
β_{xxx}	-166.18
β_{xxy}	-20.53
β_{xyy}	-158.98
β_{yyy}	-636.15
β_{xxz}	10.98
β_{xyz}	60.44
β_{yyz}	-63.36
β_{xzz}	14.07
β_{yzz}	51.91
β_{zzz}	11.58
β_0	5.886 x10^{-30} esu

*Reference Urea=0.3728 X10^{-30}esu.

CONCLUSION

In summary, a novel N-heterocyclic compound EMNTC has successfully synthesized. Both experimental techniques and theoretical methods were used to determine the structural and spectroscopic properties of compound and shows good agreement with each other. Also, molecular electrostatic potential, frontier molecular orbitals (HOMO and LUMO) and non-linear optical properties of compound were investigated by theoretical results. Molecular electrostatic potential map confirms the existence of intramolecular and intermolecular interactions. The predicted nonlinear optical (NLO) properties of the complex are much greater than those of urea. The compound is a good candidate as second-order nonlinear optical material. The charge transfer interaction has been analysed by frontier molecular orbital analysis.

REFERENCES

[1] EA Shokova; VV Kovalev. *Pharm Chem J.* **2016,** 50(2), 63-75.
[2] SM Roopan; R Sompalle. *Synth Commun*. **2016,** 46, 645–672.
[3] J Rani; S Kumar; M Saini. *Res Chem Intermed.* **2016,** 42, 6777–6804.
[4] SV Dinakaran; B Bhargavi; KK Srinivasan. *Pharm Chem.* **2012,** 4, 255–265.
[5] ES Masuda; J Schmitz. *Pulm Pharmacol Ther*. **2008,** 21, 461–467.
[6] CA Zificsak; JP Theroff; LD Aimone. *Bioorg Med Chem Lett.* **2011,** 21, 660–663.
[7] RD Sharma; S Bag; NR Tawari; MS Degani; K Goswami; MVR Reddy. *Parasitology*. **2013,** 140, 959-965.
[8] Y Zhou; T Guo; X Li; Y Dong; P Galatsis; DS Johnson; Z Pan. *Med Chem Comm*. **2014,** 5, 352–357.
[9] D Nachtigallova; M Barbatti; JJ Szymczak; P Hobza; H Lischka. *Chem Phys Lett*. **2010,** 497, 129-134.
[10] M Weinberger; F Berndt; R Mahrwald; NP Ernsting; HA Wagenknech. *J Org Chem*. **2013,** 78, 2589-2599.
[11] G Bereket; C; Ogretir; M Yama; E Hur. *J Mol Struct (THEOCHEM)*. **2003,** 625, 31-38.
[12] MS Masoud, MK Awad, MA Shaker, MMT El-tahawy. *Corros Sci*. **2010,** 52, 2387–2396.
[13] EV Verbitskiy; EM Cheprakova; JO Subbotina. *Dyes and Pigment*. **2014,** 100, 201-214.CEPTEDMANUSCRIPT
[14] J Weng; Q Mei; Q Ling; W Huang. *Tetrahedron.* **2012,** 68, 3129-3134.
[15] M Khashi; SA Beyramabadi; A Davoodnia; Z Ettehadi. *J Mol Struct.* **2017,** 1134, 789-796.
[16] I Matulkov; J Mathauserov; I Císarov; I Neme; J Fabry. *J Mol Struct*. **2016,** 103, 82-93.
[17] AD Boese; J; ML Martin. *J Phys Chem A.* **2004,** 108, 3085-3096.
[18] Q Hu; Y He; L Li. *Asian J Chem*. **2016,** 28 (6), 1244-1252.
[19] M Govindarajan; M Karabacak. *Spectrochim Acta A*. **2012,** 96, 421-435.
[20] L Fleming. Frontier Orbitals and Organic Chemical reactions, John Wiley & Sons, London, **1976.**
[21] L Sinha; O Prasad; V Narayan; SR Shukla. *J Mol Simul*. **2011,** 37(2), 153-163.
[22] DFV Lewis; C Ioannides; DV Parke. *Xenobiotica*. **1994,** 24, 401-408.
[23] B Kosar; C Albayrak. *Spectrochim. Acta A.* **2011,** 78(1), 160-167.
[24] RN Singh; P Rawat; S Sahu. *Spectrochim Acta Part A*. **2015,** 135, 1162–1168.
[25] RN Singh; P Rawat; S Sahu. *J Mol Struct.* **2013,** 123–133.
[26] RN Singh; P Rawat; S Sahu. *J Mol Struct.* **2014,** 1076, 437–445.
[27] G Socrates. Infrared and Raman Characteristic Group Frequencies, Table and Charts, 3rd edn, Wiley, Chichester, **2001.**
[28] F Jensen , Introduction to Computational Chemistry, John Wiley and Sons Ltd., West Sussex, Chapter 9,p. 309, p. 492, Chapter 6, p. 257, **2007.**
[29] K Fukui. Role of frontier orbitals in chemical reactions. *Science*. **1982,** 218, 4574, 747-754.
[30] RG Parr; LV Szentpaly; S Liu. *J Am Chem Soc.* **1999,** 121, 1922-1924.
[31] P Politzer; JS Murray. *Protein*. **1991,** 2(13).
[32] P Politzer; DG Truhler (Eds.). Chemical Applications of Atomic and Molecular Electrostatic Potentials, **1981.**
[33] C Andraud; T Brotin; C Garcia; F Pelle; P Goldner; B Bigot; A Collet. *J Am Chem Soc.* **1994,** 116, 2094-2101.
[34] VM Geskin; C Lambert; JL Bredas. *J Am Chem Soc*. **2003,** 125, 15651-15658.
[35] PV Kolinsky. *Opt Eng*. **1992,** 31, 11676-11684.
[36] DF Eaton. *Science*. **1991,** 25, 281-287.
[37] C Adant; M Dupuis; JL Bredas. *Int J Quantum Chem.* **2004,** 56, 497-507.